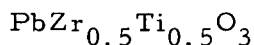


INFLUENCE OF PARTICLE SIZE AND STRUCTURE OF ZrO_2 ON MICRO-STRUCTURE DEVELOPMENT AND DIELECTRIC CONSTANT OF



K. Keizer, E. H. J. Janssen, K. J. de Vries and A. J. Burggraaf
Twente University of Technology, Department of Chemical Engineering
Laboratory of Inorganic Chemistry and Materials Science
P. O. Box 217
Enschede, The Netherlands

(Received February 26, 1973 and in final form March 28, 1973; Refereed)

ABSTRACT

The synthesis of $PbZr_{0.5}Ti_{0.5}O_3$ ceramics from the raw materials was reinvestigated in order to find relations in the characterizations for the products in various stages of the preparation procedure. Techniques used were particle size measurements, X-ray powder diffractometry, density and dielectric constant measurements and scanning electron microscopy. The results show, that the particle size and structure of ZrO_2 determine the inhomogeneity, expressed as x_T/x_R , of the calcination product. An inhomogeneous calcination product sintered at relatively low temperatures results in an inhomogeneous ceramic of low density. Using high sintering temperatures and long periods of time an inhomogeneous calcination product converts into a dense (>97%) and homogeneous ceramic.

Introduction

The electrical and optical properties of leadzirconate-titanate ceramics of a given composition, depend on quantities such as chemical homogeneity, density and average particle size. The value of each of these quantities is considered to be the result of characteristics of the raw materials as well as of the preparation conditions.

In the literature (1-11) and also in our investigations it is found, that although the same or comparable raw materials and preparation conditions are used, the resulting $PbZr_xTi_{1-x}O_3$ ceramics differ in density, particle size and electrical proper-

ties. In this literature no measuring methods are mentioned which consider the relations between product characterization of the early stages of the preparation procedure with the characteristics of an optimum ceramic in order to predict which preparation procedure has to be followed when optimum ceramics are required.

The object of our investigation is to determine whether characterizing of the intermediate phases in the preparation procedure of $\text{PbZr}_{0.5}\text{Ti}_{0.5}\text{O}_3$ ceramics can be correlated with the resulting density of the sintering procedure.

Density of considered here as the most sensitive quantity, because differences in characterization are also hereby reflected and because of a simultaneous occurrence of high density and good dielectric, ferroelectric and optical properties (1,4,9,10).

The accent in the characterization is directed at:

- the particle size and the determination of the structure in the raw materials
- the degree of chemical homogeneity and particularly the distribution of titanium and zirconium ions over B-place positions in the ABO_3 -perovskite structure after the calcining procedure
- the density of the ceramic
- the chemical homogeneity of the ceramic.

Experimental Procedure

In Table 1 structure, particle size and manufacture of the raw materials PbO , TiO_2 and ZrO_2 are given. The net purity of these materials was in all cases better than 99.5 weight % (+). 250 g batches of composition $\text{PbZr}_{0.5}\text{Ti}_{0.5}\text{O}_3$ were prepared by weighing the oxides, mixing them for 3 hrs in a roll-mill system and calcining them for 16 hrs at 850°C on an alumina support. Weight changes did not occur during this heating procedure. Chemical composition and homogeneity were characterized by means of X-ray powder diffraction (Philips diffractometer using Ni-filtered $\text{Cu-K}\alpha$ radiation) and chemical analyses (13). The calcining product was roll-milled during 3 hrs in a ceramic container. The average particle size of all powders was $3.5\mu\text{m}$. From these powders pellets of 30 g were isostatically pressed with a pressure of $3,200\text{ kg/cm}^2$

(+) The amount of impurities in the ceramics were, depending on the raw materials, between: Si, 0.02-0.15%; Mg, 0.003-0.02%; Fe, 0.02-0.04%; Al, $\leq 0.005\%$ by weight.

during five minutes. The green density thus obtained was $6.0 \pm 0.1 \text{ g/cm}^3$ or about 75% of the theoretical density of 7.98 g/cm^3 .

The pellets were sintered in platinum boxes with lead-zirconate to maintain an equilibrium pressure of PbO . The weight changes always were smaller than 0.5%. Sintering temperatures and times used were:

1. 1080°C - 1 hr
hot-pressed at
 400 kg/cm^2
2. 1180°C - 3 hrs
3. 1220°C - 3 "
- 4a. 1260°C - 3 "
- 4b. 1260°C -17.5 "
- 5a. 1280°C - 3 "
- 5b. 1280°C -17.5 "

Sintering was performed in an atmosphere of pure oxygen.

Measurements

The density of the specimens is measured by a mercury displacement method. The inaccuracy is $\pm 0.02 \text{ g/cm}^3$ (viz. 0.2%).

TABLE 1
Raw Materials

Material	Structure	Average Particle Size (μm)	Manufacture	Remarks
PbO	orthorhombic yellow	10	Merck Germany	
TiO_2	tetragonal white	2	Titan Gesell. Germany	
ZrO_2 -1	monoclinic	2	Tizon Chem. Corp. USA	
ZrO_2 -2	98% monoclinic 2% tetragonal	11	Auer Remy Germany	
ZrO_2 -3	monoclinic	11	Auer Remy Germany	heated at 1200°C
ZrO_2 -4	monoclinic	5	Auer Remy Germany	heated at 1200°C and milled
ZrO_2 -5	88% monoclinic 12% tetragonal	12	Koch-Light England	
ZrO_2 -6	94% monoclinic 6% tetragonal	3.5	Koch-Light England	milled
ZrO_2 -7	96% monoclinic 4% tetragonal	2.5	Koch-Light England	milled
ZrO_2 -8	monoclinic	6.5	Koch-Light England	heated at 1200°C and milled
ZrO_2 -9	tetragonal	1.3	wet chemical preparation	citrate method

As Table 1 shows ZrO_2 can consist of two structures. Their ratio is determined by measuring the intensities of the 111-reflections.

At room temperature the calcining product $\text{PbZr}_x\text{Ti}_{1-x}\text{O}_3$ usually consists of a mixture of two perovskite phases, a tetragonal one with $x < 0.52$ and a rhombohedral one for $0.52 < x < 0.95$. The composition of the phases are characterized by x_T and x_R respectively. Sometimes two tetragonal phases characterized by x_{T1} and x_{T2} are present. Analyses of the composition of the calcining products are based on measuring the 200-reflections for $x_R \leq 0.7$ and on measuring the 220 or 110-reflections for $x_R > 0.7$ is. Analysis of the composition of the tetragonal phase is performed by measuring the difference in d-value, according to:

$$d_{002} - d_{200} = \frac{1}{2} (c-a)$$

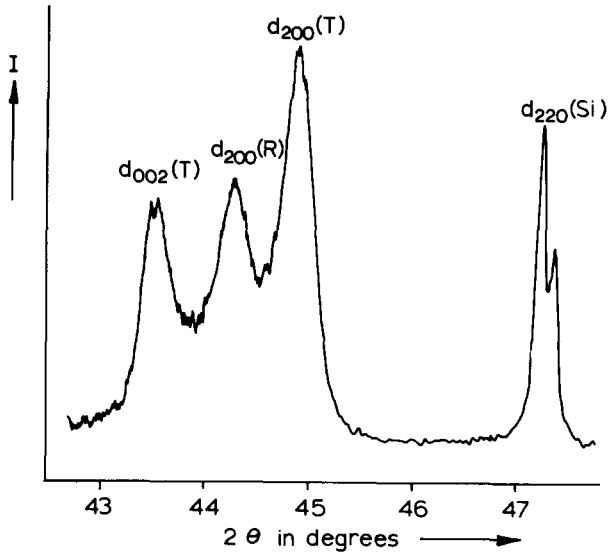


FIG. 1

The diffractometer trace of the 200-reflections of sample 1 in Table 4.

The composition of the rhombohedral phase is determined from the difference in d-value between $d_{200} - d_{220\text{Si}}$ ($d_{220\text{Si}}$ being the 220-reflection of silicon). Therefore testing curves are used. For these curves homogeneous samples are made with tetragonal and rhombohedral compositions respectively. Their compositions are determined by analytical methods. d-Values, calculated from literature values (5,8) of lattice parameters, are also used in these curves. With the least squares method the standard deviations in the testing curves are calculated and are 1.3% and 2.4% of x for the tetragonal and rhombohedral phases respectively. The weight percentages of the phases are determined from testing curves which are based on intensity relations between the reflections. The standard deviations in the weight percentages are 3-4%.

In Fig. 1 a part of the diffractometer trace of sample 1 in Table 4 is given. This part consists of the 002-reflection and 200-reflection of the tetragonal phase, the 200-reflection of the rhombohedral phase and the 220-reflection of the silicon standard sample. The values of x_T and x_R of this sample are 0.495 and 0.60 respectively. The diffractometer traces of all the other samples with one tetragonal and one rhombohedral phase are of the same type.

The determination of the particle size distribution in the powders is performed by the Whitby sedimentation method (14). These sizes are controlled by a scanning electron microscope (type Jeol JSM3) technique which shows a systematic deviation of +20% in the determinations of the sedimentation technique. The grain sizes of the ceramics are measured by the surface diameter distribution with a Zeiss TGZ-3 according to Endter. Comparison of the particle

The composition of the rhombohedral phase is determined from the difference in d-value between $d_{200} - d_{220\text{Si}}$ ($d_{220\text{Si}}$ being the 220-reflection of silicon). Therefore testing curves are used. For these curves homogeneous samples are made with tetragonal and rhombohedral compositions respectively. Their compositions are determined by analytical methods. d-Values, calculated from literature values (5,8) of lattice parameters, are also used in these curves. With the least squares method the standard deviations in the testing curves are calculated and are 1.3% and 2.4% of x for the tetragonal and rhombohedral phases respectively. The weight percentages of the phases are determined from testing curves which are based on intensity relations between the reflections. The standard deviations in the weight percentages are 3-4%.

sizes before and after the sintering procedure is very difficult and not performed because of differences in measuring techniques.

Dielectric constant (ϵ') measurements at 10 and 100 kc/s as a function of temperature are used for the determination of the ferro-electric para-electric transition. The samples are provided with gold evaporated electrodes. A Wayne Kerr Universal Bridge, type B221 and a resonance bridge according to Ismailzade (15) are used for the measurements.

Results

Calcining products

Differences in particle sizes of TiO_2 and PbO show a negligible effect on the homogeneity of the calcining product compared to differences in ZrO_2 . Therefore our results are only concerned with the influence of differences in ZrO_2 . These differences are expressed as: a) the average particle size, b) the structure composition in weight % monoclinic and tetragonal.

In Fig. 2 the influence of the particle size of pure monoclinic ZrO_2 is shown as a function of x_T and x_R of the calcining product. Extrapolation of the curves for x_T and x_R to particle sizes smaller than $2\mu\text{m}$ show that these curves do not intersect at the aimed composition $\text{PbZr}_{0.5}\text{Ti}_{0.5}\text{O}_3$. The mole fraction of the rhombohedral phase x_R is different at each composition and is smaller when x_R is smaller. At $x_R = 0.58-0.60$ the mole fraction of x_R tends towards zero and the mole fraction of x_T towards one. The found calcining products only consist of the perovskite phases as was detected by X-ray diffraction.

In Table 2 the effect of the structure composition of ZrO_2 powders on x_T and x_R is shown. ZrO_2 powders consisting of two structures with particle sizes larger than $3\mu\text{m}$ result in the highest inhomogeneous calcining products viz. x_T/x_R is small. With average particle sizes of about $10-12\mu\text{m}$ these powders result in calcination products with a broadened tetragonal composition. For pure tetragonal ZrO_2 no relation is found between the composition of the calcining product and the particle size of this ZrO_2 powder. The reason for this is, that a wet (citric acid) chemical method is used to obtain the tetragonal phase, which method only gives small particle sizes. Also a constant ratio of tetragonal to tetragonal+monoclinic at various particle sizes is not

used because this ratio is a function of the grinding procedure.

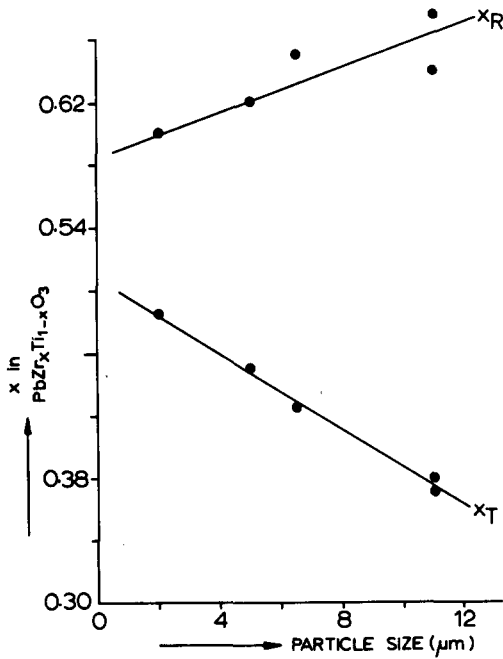


FIG. 2

Composition of the solid state reaction product as a function of the particle size of monoclinic ZrO_2 .

TABLE 2

Influence of ZrO_2 on the Composition of the Calcining Products.

type of ZrO_2 (see Table 1)	chemical composition of $PbZr_xTi_{1-x}O_3$			weight percentages of the phases		
	x_{T1}	x_{T2}	x_R	x_{T1}	x_{T2}	x_R
ZrO_2 -2	0.15	0.48	0.69 ⁵	20	30	50
ZrO_2 -5	0.15	0.45	0.71	20	30	50
ZrO_2 -6	-	0.44	0.61 ⁵	-	65	35
ZrO_2 -7	-	0.48 ⁵	0.54 ⁵	-	70	30
ZrO_2 -9	-	0.51	0.52	-	80	20

These results show that differences in particle size and structure composition have a decisive influence on homogeneity of the calcining product.

Sintering

In Fig. 3 the density obtained under different conditions is given as a function of particle size of monoclinic ZrO_2 . It appears that at sintering temperatures of about $1220^{\circ}C$ the density decreases with an increase in particle size. The reproducibility of the density decreases with increasing particle size. At $1260^{\circ}C$ and $1280^{\circ}C$ and sintering times of 17.5 hours the density is almost independent of the particle size of ZrO_2 .

In Fig. 4

the relation between inhomogeneity parameters (expressed as x_T/x_R) and the density is given. This relation is of the same type as that between the particle size of ZrO_2 and the density.

However, the relationship in Fig. 4 is better for characterization of the influence of the sintering procedure, because there is no detectable ZrO_2 present in the calcining product.

When in the calcining product besides the rhombohedral phase more than one tetragonal phase is found, the density is very low (Table 3 and Fig. 4). Pure tetragonal ZrO_2 always results in a very homogeneous calcining product and therefore in a

high density at a low (e.g. 1220°C) sintering temperature (Tables 1-3).

The degree of inhomogeneity of the calcining product as determined from X-ray diffractometry (x_T/x_R being a measure for the distribution of zirconium and titanium ions over the B-place position in ABO_3) determines the sintering procedure to be followed when a certain density is required.

It is found, that microstructure is a function both of particle size distribution and average particle size of the calcining products and of sintering conditions. Table 3 shows the influence of the sintering conditions. After sintering, the inhomogeneity of the calcining product does not show to have any influence on the grain size of the ceramic. The distribution function of the grain size of the ceramic agrees with a log-normal distribution and the deviation is 1.6 ± 0.1 .

An example of the microstructure by scanning electron microscopy is given in Fig. 5. It shows that pores occur at grain boundaries.

Starting with calcining products of various inhomogeneities, it is found, that after a sintering procedure carried out in order to obtain dense ceramics, all X-ray detectable inhom-

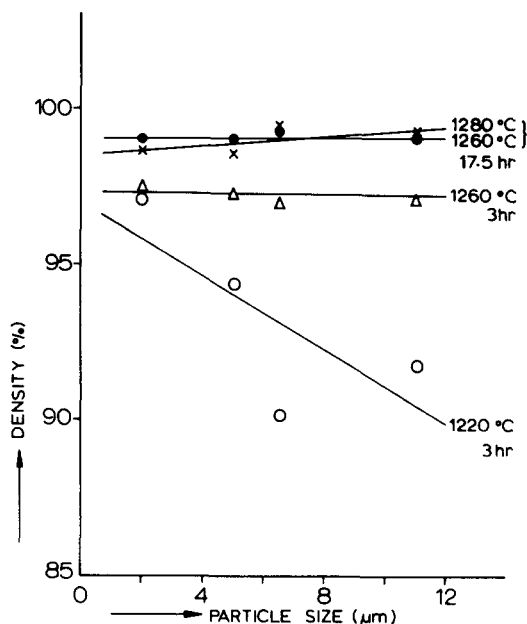


FIG. 3

The density of $\text{PbZr}_{0.5}\text{Ti}_{0.5}\text{O}_3$ as a function of the particle size of monoclinic ZrO_2 .

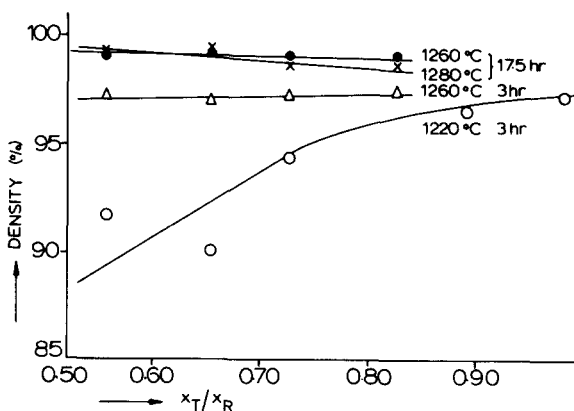


FIG. 4

The density of $\text{PbZr}_{0.5}\text{Ti}_{0.5}\text{O}_3$ as a function of the inhomogeneity parameter x_T/x_R .

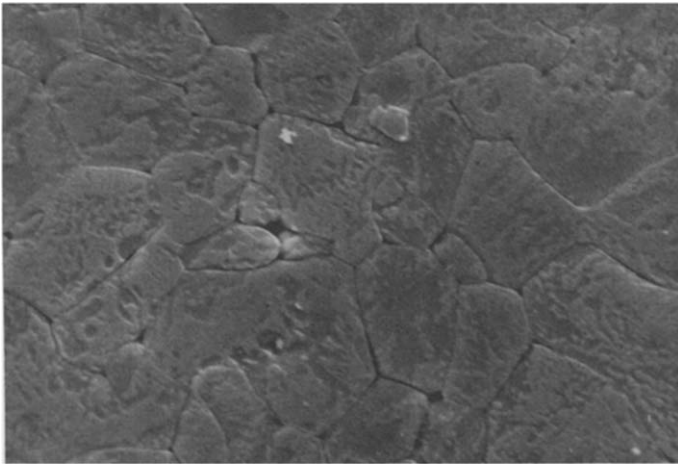


FIG. 5

The microstructure of a sintered $PbZr_{0.5}Ti_{0.5}O_3$ ceramic (sample 4 in Table 4, magnification 3,600x).

TABLE 3

Relations between the Phase Composition of $PbZr_xTi_{1-x}O_3$ and the Microstructure of the Ceramics.

composition chem. comp.			calcining product weight perc.			sint. conditions	density %	average particle size (µm)	
x_{T1}	x_{T2}	x_R	x_{T1}	x_{T2}	x_R				
0.15	0.48	0.69 ⁵	20	20	60	1	95.5	2	
						3	81.6	1.9	
						4 ^a	89	2.2	
						4 ^b	96	3.9	
0.15	0.45	0.71	20	30	50	5 ^b	98.6	3.6	
						3	97		
		0.51	0.52		80	20	4 ^a	97.2	
		0.42 ⁵	0.65		70	30	4 ^b	99.2	4.0
		0.45	0.62	70	30	3	94.3	1.4	
	5 ^a					96.1	2.4		
	5 ^b					98.5	3.2		
		0.48 ⁵	0.59 ⁵		80	20	4 ^b	99	3.2

geneities have vanished. A second phase besides the perovskite phase could only be detected by a scanning electron microscope and the microprobe analyzer. The second phase has the form of nodules. They are composed of silicon and zircon oxides. This silicon is already present as an impurity in the raw materials and further derived during the milling processes. In order to cheque if the zircon oxide combined with silicon-oxide in the nodules, release a corresponding amount of PbO in the lattice, about 0.4 weight % of SiO_2 is added to the starting composition prior to the preparation procedure. The nodules are found again, but now surrounded by a Pb-Si phase. In the bulk of the perovskite no silicon can be de-

tected, while the amount of unreacted PbO is increased. The compositions of the ceramics are analysed after applying the extraction method of Robinson and Joyce (16) on unreacted oxides. This extraction method was unsuitable for our materials, because not only unreacted PbO but also PbO combined in $PbZr_xTi_{1-x}O_3$ was extracted. New methods are being developed, which will be published separately.

The method of analyzing the distribution of zirconium and titanium ions over B-place positions show, that the reaction sequence in the calcining procedure is different from the sequence proposed by Matsuo and Sasaki (18). This point is raised again in a following paper. It appears possible to apply the distribution analyzing method also to lanthana-doped lead zirconate-titanate. The propositions are, that at room temperature measurable differences occur in the axes ratio c/a , whereas the measurements have to be fulfilled for compositions near the morphotropic phase boundary in this system.

Dielectric constant

Tablets made from the sintering products are heated for 2 hours at 900°C in pure oxygen in order to eliminate both grinding and polishing traces and uncombined PbO [Härdtl et al. (19)]. The ferro-electric transition is determined from measurement of the dielectric constant ϵ' as a function of the temperature at 10 kc/s and 100 kc/s. The results for 10 kc/s and 100 kc/s are almost the same. In Table 4 the values are given of the Curie temperature (T_C), the maximum of ϵ' and the maximum of ϵ' after correction for porosity according to Looyenga (17) by using the relation:

$$V_{\text{por}} = \frac{\epsilon'_m{}^{1/3} - \epsilon'_{\text{bulk}}{}^{1/3}}{\epsilon'_{\text{por}}{}^{1/3} - \epsilon'_{\text{bulk}}{}^{1/3}}$$

Here V_{por} = the fraction of volume of the pores; $\epsilon'_m = \epsilon'$ of the sample; $\epsilon'_{\text{por}} = \epsilon'$ of vacuum or air, being 1; $\epsilon'_{\text{bulk}} = \epsilon'$ of the material without pores.

In Fig. 6 ϵ' versus T curves of the ferro-electric para-electric transition are shown from samples (see Table 4) obtained under various sintering conditions. The absolute values of $\epsilon'_{\text{max(bulk)}}$ given in Table 4 may be influenced to some extent by the porosity correction procedure. Therefore these values are used in a qualitative way. Decrease of the overall-Curie temperature (T_C) and a simultaneous increase of the maximum value of $\epsilon'_{\text{max(bulk)}}$ seem to be a measure for the progress of the homogeneity of the ceramic. Comparing the results of Fig. 6 and Table 4 with the results of

TABLE 4
Relation between Sintering Conditions, Resulting Microstructure and the Ferro-electric Transition Temperature

number	composition ceramic	average particle size	density (%)	T_c	$\epsilon'_{max} \cdot 10^3$ (meas.)	$\epsilon'_{max} \cdot 10^3$ (bulk)
1	$x_T = 0.495$ (80 weight%) $x_R = 0.60$ (20 weight%)	2	95.5	414 ± 2	15.9	18.3
2	$x_T = 0.50$	3.9	96.0	402 ± 2	29.6	33.5
3	$x_T = 0.50$	1.9	81.6	412 ± 2	11.4	21.0
4	$x_T = 0.50$	3.2	99.0	402 ± 2	22.1	22.8

The sample numbers 1 to 4 correspond to the sinterconditions 1,4b,3 and 4b, resp. as given in Table 3. They differ in density.

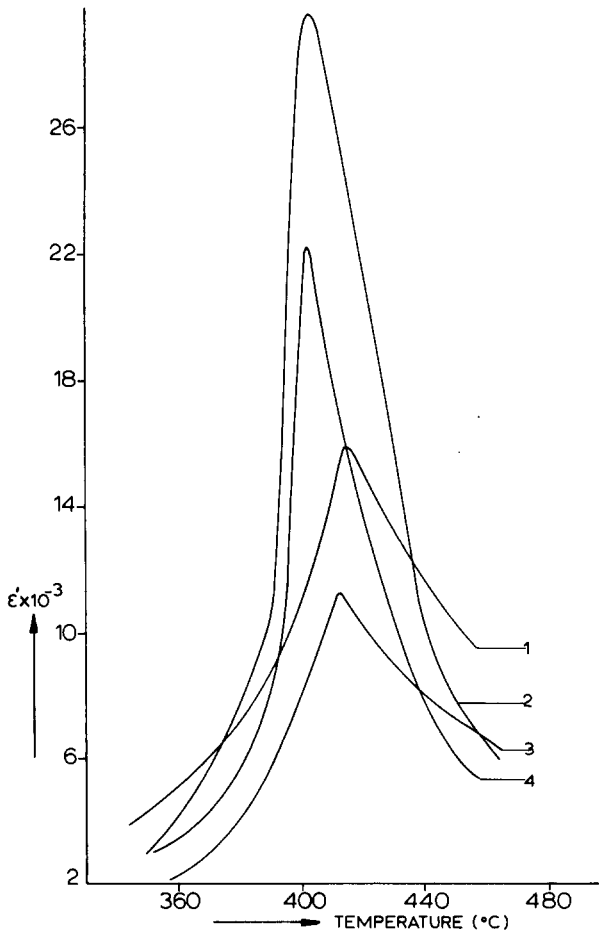


FIG. 6
Dielectric constant ϵ' as a function of the temperature at 10 kc/s. The number 1-4 correspond to the number 1-4 in Table 4.

the X-ray powder diffractometry, these do suggest that for our materials dielectric measurements around the Curie temperature still reveal differences in degree of homogeneity of the four samples when X-ray diffractometry does

not. It appears from Table 4 that Curie temperature of our samples are $8^\circ C - 20^\circ C$ higher than values mentioned in the literature (5,8) viz. $394^\circ C \pm 1^\circ C$. These differences are considered to be significant since our measurements have an inaccuracy of $\pm 2^\circ C$.

Hence we conclude that the ceramics mentioned in literature (5,8) have a higher degree of homogeneity than ours. This seems to be a reasonable conclusion because Hårdtl (18) used sintering temperatures of 1300° and Weirauch (5) sintered his samples three times between $1000^\circ C$ and $1300^\circ C$ with milling procedures in between. Both these type of manipulations furthered the homogeneity

of the samples.

In Table 4 the samples have optimal ϵ'_{max} values at densities lower than 99 %. This behaviour can also be found by comparing the results of Weirauch (5) $\epsilon'_{\text{max(meas.)}} = 34 \times 10^3$ by a density of 90 % and Hårdtl (8) $\epsilon'_{\text{max(meas.)}} = 19.4 \times 10^3$ by a density of 99 %. The reason for this is not yet clear but can not be attributed to a difference in grain size, which is only 0.7 μm .

Conclusions

The particle size of monoclinic ZrO_2 is of principal interest for the degree of inhomogeneity of the calcining product. The larger the particle size of ZrO_2 is, the smaller the ratio $x_{\text{T}}/x_{\text{R}}$ will be. When ZrO_2 also contains a tetragonal structure this influences $x_{\text{T}}/x_{\text{R}}$ in the same sense but to a lesser degree than the particle size does. A small ratio of $x_{\text{T}}/x_{\text{R}}$ causes a low density (viz. high porosity) at low sintering temperatures.

It is not necessary to start from a homogeneous calcining product when a dense ceramic is required. The choice of the sintering conditions based on the characterization of the calcining product insures densities of 97 % and better. The average grain size in the ceramic is mainly determined by sintering temperatures and times.

The shape and place of the ϵ' versus temperature curves at the ferro-electric para-electric transition appear to be more sensitive to inhomogeneities in the ceramics than X-ray diffraction techniques do.

References

1. P.D. Levett, Am.Cer.Soc.Bull. 42, 348 (1963).
2. R. Geesemann and H. Neels, Hermsd.Techn.Mitt. 12, 339 (1965).
3. Y. Tanada, T. Ikeda and H. Toyoda, Rev.Elec.Comm.Lab. 13, 744 (1965).
4. G.H. Haertling, Am.Cer.Soc.Bull. 49, 564 (1970).
5. D.F. Weirauch, Ph.D.Thesis, University of Illinois, Urbana (1968).
6. G.A. Pryor, M.S. Thesis, Univ. of Calif., Berkely (1968).
7. R.B. Atkin, J.Am.Cer.Soc. 54, 265 (1971).
8. K.H. Hårdtl, private communication.

9. K. Carl and K.H. Härdtl, *Ber. Deut.Keram.Ges.* 47, 681 (1970).
10. A.M. Webster, T.B. Weston and V.M. McNamara, *J.Can.Ceram. Soc.* 35, 61 (1960).
11. D.A. Buckner and P.D. Wilcox, *Am.Cer.Soc.Bull.* 51, 218 (1972).
12. J. Bailey, D. Lewis, Z.Li.Brant and J. Porter, *J. Brit. Cer.Soc.* 71, 25 (1972).
13. J.H.H.G. van Willigen, *Anal.Chim.Acta* 62, 279 (1972).
14. K.T. Whitby, *Heating, Piping and Air Conditioning* 61, 449 (1955).
15. J.G. Ismailzade, *Sov.Phys.Cryst.* 12, 625 (1968).
16. A. Robinson and T. Joyce, *Trans.Brit.Cer.Soc.* 61, 85 (1962).
17. H. Looyenga, *Physica* 31, 401 (1965).
18. Y. Matsuo and H. Sasaki, *J.Am.Cer.Soc.* 48, 289 (1965).
19. K.H. Härdtl and D. Hennings, *J.Am.Cer.Soc.* 55, 230 (1972).